Journal of Thermal Analysis and Calorimetry, Vol. 80 (2005) 541–548

FLAME PROPAGATION OVER LIQUID ALCOHOLS
Part I. Experimental results

E. Degroote[1*] *and P. L. García Ybarra*[2]

[1]Universidad Politécnica de Madrid, Dep. Ciencia y Tecnología Aplicadas, E. U. I. T. Agrícolas, Ciudad Universitaria, s/n. 28040 Madrid, Spain
[2]CIEMAT, Av. Complutense, 22, 28040 Madrid, Spain

The different spreading regimes above liquid fuels have been experimentally described for a wide range of initial surface temperatures. Five different spreading regimes are observed. The flame spreading driving parameter has been found. The critical transition temperatures between these regimes have been characterized; they present common characteristics for the four alcohols (methanol, ethanol, propanol and butanol) used in the experiments. A preheating zone ahead of the flame (produced by thermocapillarity) has been observed. The initial surface temperature of the liquid fuel results to be a control parameter of flame spreading; therefore, it can be applied to improve fire safety conditions in fuel containers.

Keywords: *combustion, flame spreading, fuels, heat transfer, temperature*

Introduction

Flame spreading over liquid fuels has been the subject of several works. Akita [1] described the basic features of the flame spreading velocity (v_f), and some computer codes have been developed for this propagation mode [2–4]. In spite of this, the experimental characterization of the process is still incomplete; furthermore, the nature of the basic mechanisms involved has been the object of discussion in fundamental points [5–11]. The purpose of this work is to contribute to the experimental study of the different regimes of flame spreading over liquid fuels when the temperature of the liquid phase is kept uniformly at some initial value T_0.

Experimental

The experimental setup consists of an open channel configuration, filled with a liquid fuel. The initial fuel temperature T_0 was kept uniform along the horizontal with a refrigerant circuit. Four aliphatic alcohols (methanol, ethanol, 2-propanol and 1-butanol) and two different channel lengths have been used (40×4.0×2.5 and 100×1.5×3.4 cm, respectively). Additionally, two different kinds of lateral walls were employed (aluminium and Pyrex). The whole channel was covered by a thin metallic net to reduce the influence of air currents on the flame spreading. The distance from the channel to the net was approximately 30 cm. The room temperature was nearly constant, close to 21ºC. The gas mixture was ignited at one end of the channel and the spreading observed until the flame reached the other end.

Eight thermocouples (Cr–Al, ϕ=25 μm), regularly spaced along the central line of the fuel surface, record the evolution of the fuel surface temperature (sampling rate N=1 kHz). The thermocouples wires enter laterally from the top towards the bottom of the channel. After reaching the central part of the channel section, they arrive (from the bottom) very close to the liquid surface. In this way only the tips of the thermocouples were located in the liquid in the vicinity of the surface. The estimated distance between the thermocouples and the liquid surface is, approximately, 50 μm. Therefore, the influence of the wires on flame spreading is dramatically reduced.

The voltage generated by the temperature differences between the two welds in the thermocouple was amplified by a factor of 10^3 using an EXP-16 amplification card (Metrabyte). The data were collected on a PC computer by a DASH-16 AD/DA acquisition card (Metrabyte). The estimated error on the temperature measurement did not exceed 0.1ºC.

Also, using a composite image technique, a video camera provides (in almost complete darkness) records of the flame front evolution (x_f) along the central line of the channel for each value of T_0. By using a simple numerical derivation method, the spreading velocity of the flame can be calculated and (v_f) can be represented as a function of T_0 as a bifurcation diagram. Using these data, we can also plot the phase diagram. The complete scheme of the experiment is shown in Fig. 1.

* Author for correspondence: eugenio.degroote@upm.es

1388–6150/$20.00

Akadémiai Kiadó, Budapest, Hungary
Springer, Dordrecht, The Netherlands

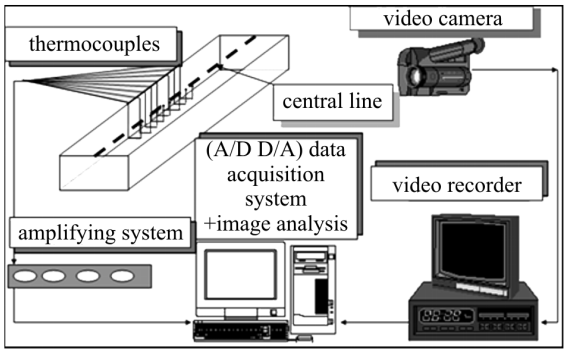

Fig. 1 Experimental setup

Unless otherwise specified, the results given in this paper correspond to experiments carried out on the larger channel for ethanol (qualitatively identical results have been observed for all of the alcohols and channels).

Results

Flame front position

From the direct video recording, a measurement of the spreading position (x_f) can be made at any location along the channel. For each video image, we select the geometric line corresponding to the channel's central line. Using a color decoder (DEC-110-P), and after a RGB decomposition, we only digitize the blue color intensity with a PC computer ATVista-Truevision imaging board. The line presents then three different regions: a dark region (which corresponds to the unburnt side), a coloured region (which corresponds to the burnt zone) and a third region between the two previous ones (which corresponds to flame front position). The lines obtained for successive times are pasted to obtain a composite image. On this composite image, the line separating the dark region and the coloured region is the flame front position as a function of time. The resulting dividing line for the flame spreading is represented by the dotted line in Figs 2–5.

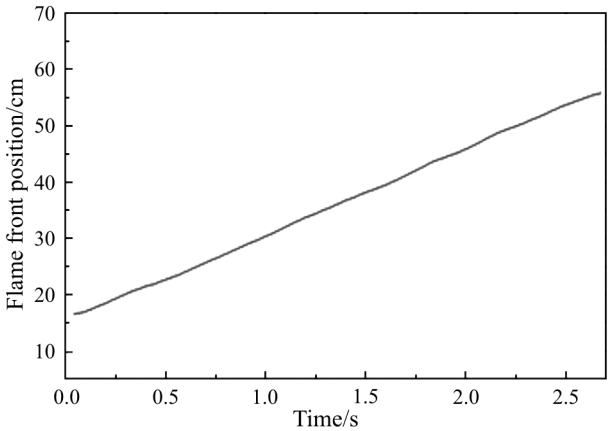

Fig. 2 Flame front evolution (T_0=6.7ºC)

Uniform regime

For temperatures $T_0>T_3$, being T_3 a critical temperature of the system, flame spreading is uniform. Flame velocities vary from 15 cm s^{-1} (when T_0 is close to T_3=5.8ºC) to 65 cm s^{-1} (for T_0=17.3ºC). Figure 2 shows a typical run in this region.

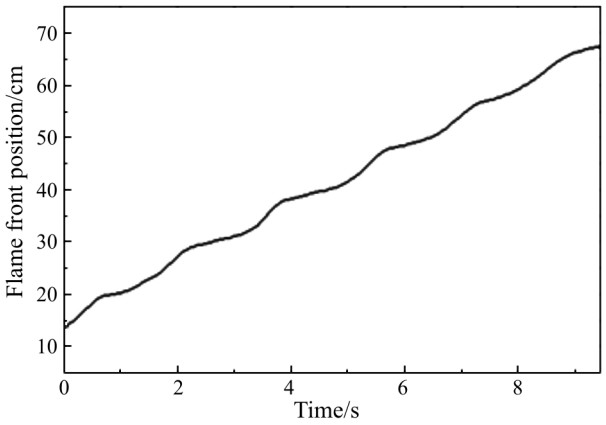

Fig. 3 Flame front evolution (T_0=–0.5ºC)

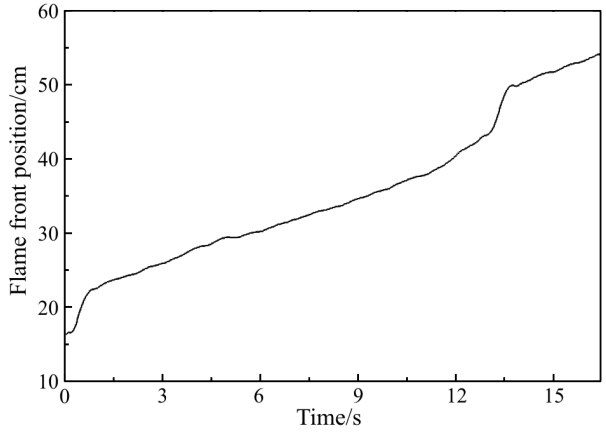

Fig. 4 Flame front evolution (T_0=–9.2ºC)

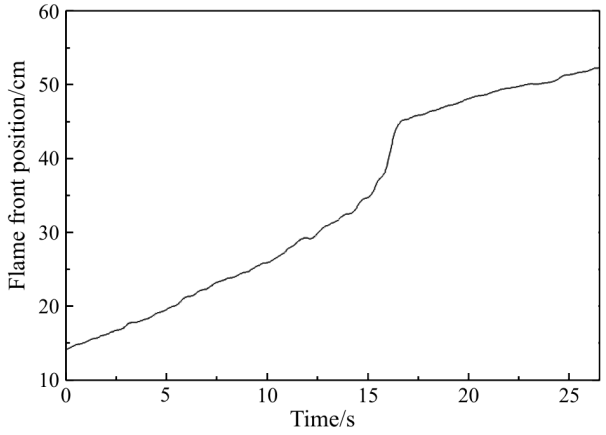

Fig. 5 Flame front evolution (T_0=–14.3ºC)

Pulsating regime

For temperatures $T_0<T_3$, the flame exhibits an oscillatory behavior. Slow motion periods are followed by quick motion periods, and so on, as it can be seen in Fig. 3. In this case regime (that is, for values of T_0 close to T_3) the oscillations are quite regular.

But, as we decrease T_0, the oscillatory spreading behaves in a more complicated manner. For lower temperatures the flame front progress is slow most of the time, but presents periodic bursts of rapid propagation, as shown in Figs 4 and 5. Mean velocity (the mean slope of the curves) also decreases with the temperature.

Pseudo-uniform regime

Finally, for lower surface temperatures $T_0<T_4<T_3$, the oscillatory spreading disappears; it cannot be detected any longer, even for very large periods of time. Instead of the pulsation mechanism observed before, a steady flame propagation regime of low velocity (of order 1 cm s^{-1}) appears. It is important to notice that this regime exists for a very significant range of temperature: the temperature T_4 does not correspond with the transition to a non-flammable regime. The transition temperature T_5 to this kind of extinction regime (where $v_f<0$) should correspond to much lower temperatures. Figure 6 is a typical plot in this region.

Flame front velocity

The flame front evolution is used to derive the instantaneous flame spreading velocity. Figures 7 and 8 depict the velocity profiles for two different values of T_0 in the pulsating regime. The first temperature (T_0=–2.0ºC) is close to the critical value T_3.

The second temperature (T_0=–14.3°C) is very close to the transition temperature to the pseudo-uniform region.

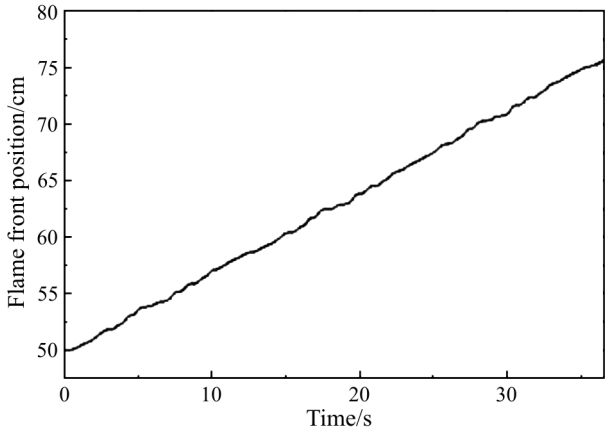

Fig. 6 Flame front evolution (T_0=–15.6ºC)

Finally, Fig. 9 shows the corresponding plot in the pseudo-uniform region. The graphic has been observed for the temperature T_0=–15.6ºC.

Only a few measurement points were obtained in this region, but the results are very clear. This fact is a direct consequence of our experimental setup: the thermalizing system could not reach values of T_0 lower than –17.5ºC.

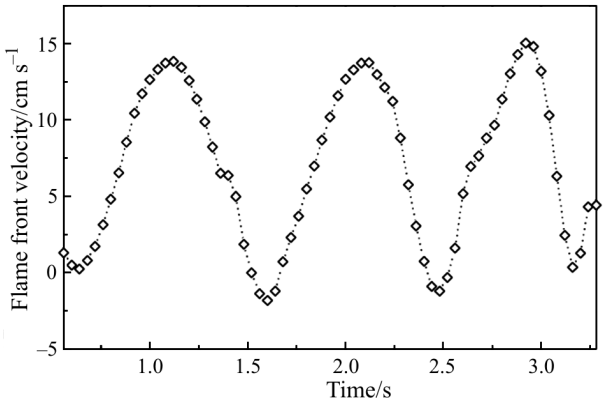

Fig. 7 Flame front velocity (T_0=–2.0ºC)

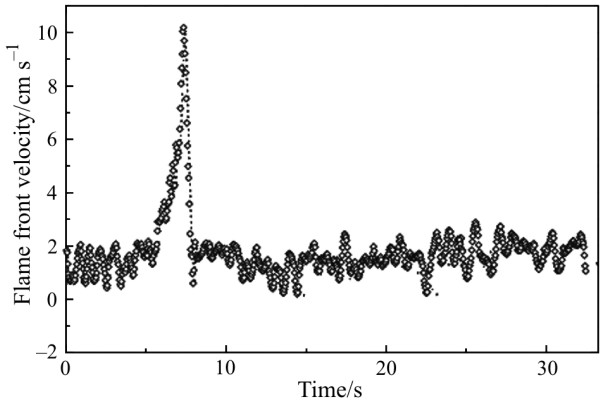

Fig. 8 Flame front velocity (T_0=–14.3ºC)

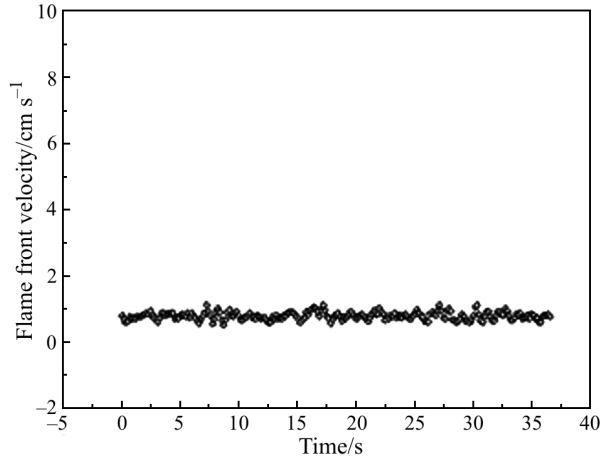

Fig. 9 Flame front velocity (T_0=–15.6ºC)

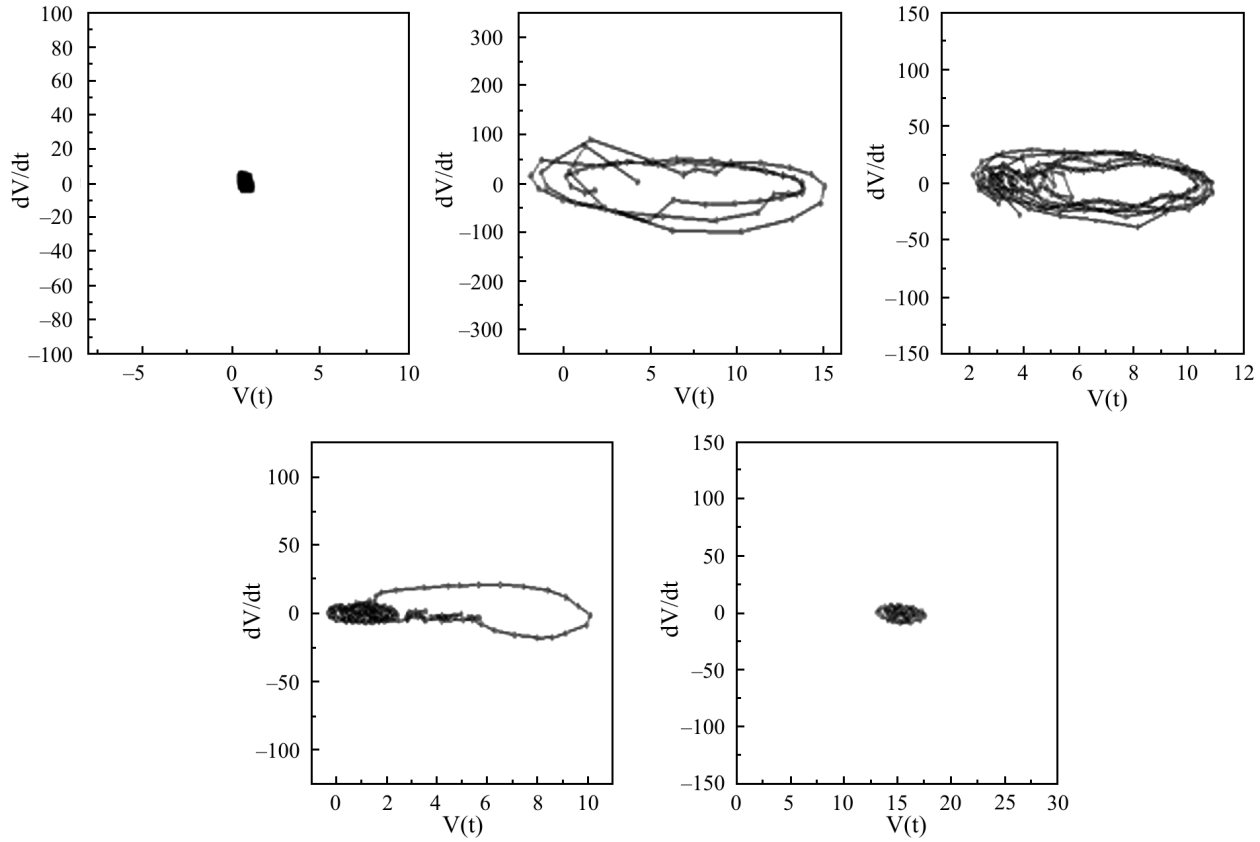

Fig. 10 Phase diagram

Phase diagram

We can also plot the phase diagram of the flame velocity (v_f); Fig. 10 gives the phase diagram for five different values of T_0 (the x-axis represents v_f, the y-axis represents its derivative, dv_f/dt). The first one corresponds to the uniform region; the second graphics corresponds to the pulsating region for a temperature close to T_3. The third graphic is in the middle of the oscillatory regime and the fourth picture has been obtained for a temperature close to T_4. Finally, the last diagram has been obtained in the pseudo-uniform zone.

Bifurcation diagram

We can register the maximum and the minimum spreading velocity of the flame obtained during every record interval. They are represented in Fig. 11 as a function of the initial liquid surface temperature (squares represent maximum spreading velocities; diamonds are the minimum velocities). The different spreading regimes described in the previous sections are clearly identified. As shown by the figure:

- For large values of the initial surface temperature $T_0>T_1$, being T_1 a critical temperature the fuel vapor pressure is so high that it leads to a flame spreading regime purely controlled by the gas phase, where the presence of the liquid fuel is ignored by the flame. Flame propagation velocities of the order of 100 cm s^{-1} are observed in this region.
- For relatively high temperatures $T_2<T_0<T_1$, v_f vary from the order of 100 to approximately 15 cm s^{-1}, v_f (and the logarithm of v_f as well) decrease, almost linearly, with decreasing temperatures, with a slope of the order of 10 cm s^{-1} $^oC^{-1}$.

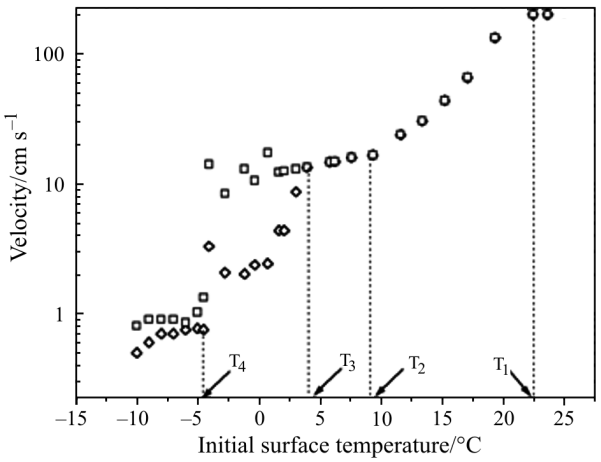

Fig. 11 Bifurcation diagram for the spreading of flames over liquid ethanol for the 100 cm long channel

- For lower temperatures $T_3<T_0<T_2$, flame spreading is still uniform, but in this case the slope of the T_0–v_f diagram is of order 1 cm s^{-1} $^oC^{-1}$, then showing a sharp transition with respect to the preceding regime.
- For even lower temperatures $T_4<T_0<T_3$, the flame spreading exhibits oscillatory behavior.
- For temperatures $T_0<T_4$, flame spreading velocity is almost constant, with values close to 1 cm s^{-1}.

Oscillation period

The period of the oscillations in the pulsating regime is shown in Fig. 12 as a function of the initial fuel surface temperature T_0. The experimental data fit with the logarithmic curve

$$P = \log\left(\frac{T_0 - T_4}{T_4}\right)$$

where the period diverges for $T_0=T_4$.

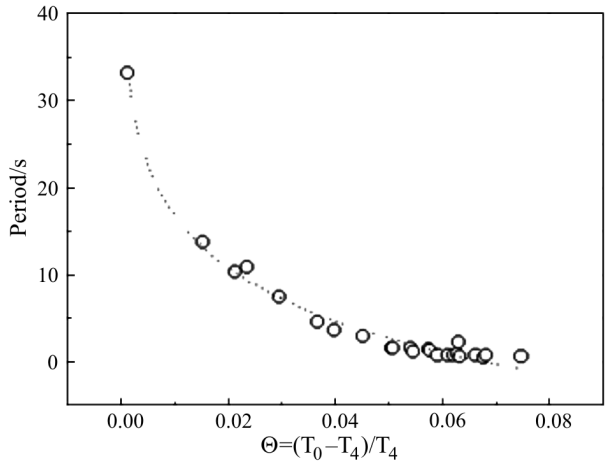

Fig. 12 Oscillation period *vs*. initial fuel surface temperature

Surface temperature evolution

The thermocouples record an abrupt increase of the liquid surface temperature, as the flame arrives at the thermocouple location. Figure 13 shows a typical run for uniform flame spreading.

It is clear, from this figure, that the time lag between temperatures increases for consecutive thermocouples (which are located 4 cm apart) is constant, indicating a uniform flame spreading regime. For values $T_2<T_0<T_3$ we can observe that there is a slight increase preceding the flame arrival. This small temperature increase is the proof of the existence of a surface flow in front of the flame, which modifies its spreading. The large temperature gradients induced in the liquid phase create a vortex that moves with the flame at some characteristic velocity) (u_s), which heats up the fluid ahead of *ii*. This is a distinctive characteristic

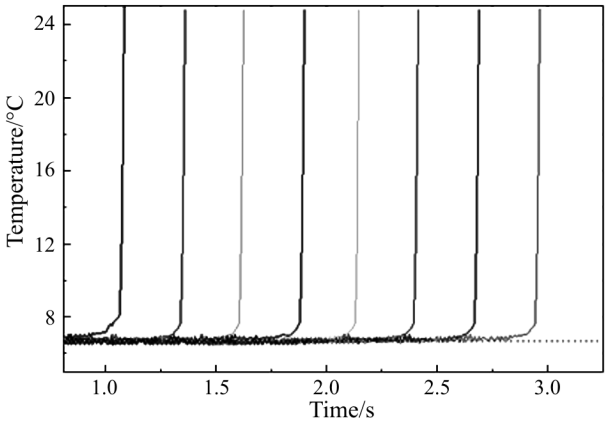

Fig. 13 Detail of the thermocouple reading for T_0=6.7ºC

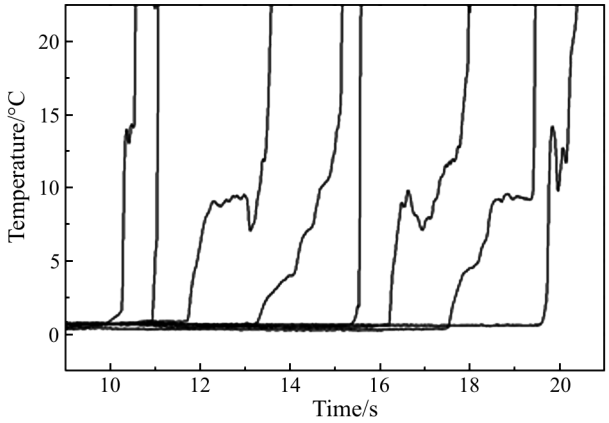

Fig. 14 Detail of the thermocouple reading for T_0=0.7ºC

of flame spreading over liquid fuels with the solid case, where no convection can be produced. The vortex structure is fundamental in the liquid case, as Fig. 14 shows. This plot corresponds to the pulsating region, for a temperature close to T_3.

We can observe fast motion periods (with a small preheated region) that lead to slow motion periods (with a bigger preheated region). When the vortex is built up ahead of the flame, the enriched gas mixture increases the flame spreading velocity: the flame advances quickly through the gas up to the limit border of the vortex (fast motion period), where the gas mixture is colder. The propagation velocity is therefore reduced (slow motion period) and a new preheated region is rebuilt as before. After some induction time, the vortex is built up again and the process restarts (fast motion period).

This process can also be observed in Fig. 15, where the initial fuel surface temperature is close to T_4.

Finally, for $T_0<T_4$, the oscillation disappears; although a large preheated region has been built up, no fast motion period is observed, and a slow motion (of order 1 cm s^{-1}) is registered.

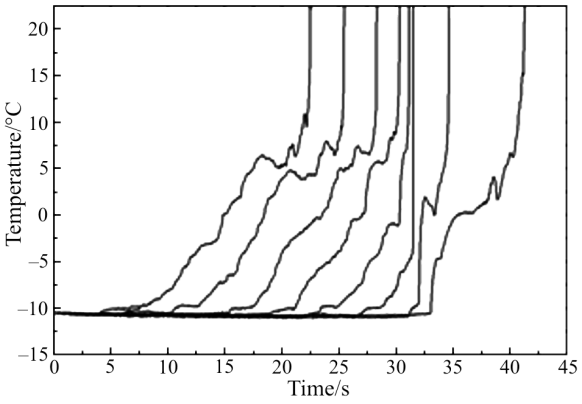

Fig. 15 Detail of the thermocouple reading for T_0=–10.6ºC

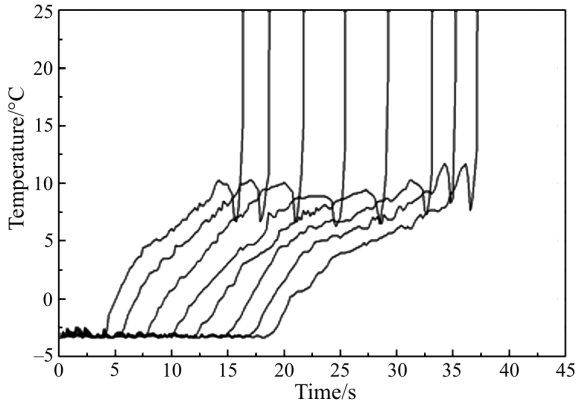

Fig. 16 Detail of the thermocouple reading for T_0= –3.1ºC (propanol, 40 cm long channel)

A typical plot in this region is presented in Fig. 16, which corresponds to butanol in a 40 cm long channel (the distance between thermocouples is now 2 cm). The mean flame velocities between thermocouples are close to 0.8 cm s^{-1}. The preheating starts at the first thermocouple location 12.3 s before the flame arrival. Therefore, in this case, the characteristic length of this region is of order 10 cm. Similar results are found for the remaining thermocouples.

Thermocapillary convection zone

In spite of the limited accuracy of the temperature measurement technique (surface thermocouples), an approximate measure of the horizontal length L of this preheat region *vs*. the initial fuel temperature is shown in Fig. 17. No detectable increase has been observed for $T_0>T_2$. For $T_3<T_0<T_2$ a small preheated region is observed, of order 1 cm; these results agree with previous works [5, 6] in this region where, by using interferometry and rainbow-Schlieren techniques, a small vortex is observed. For $T_4<T_0<T_3$, a well developed vortex appears. Finally, the characteristic length of the vortex in the pseudo-uniform region is almost constant.

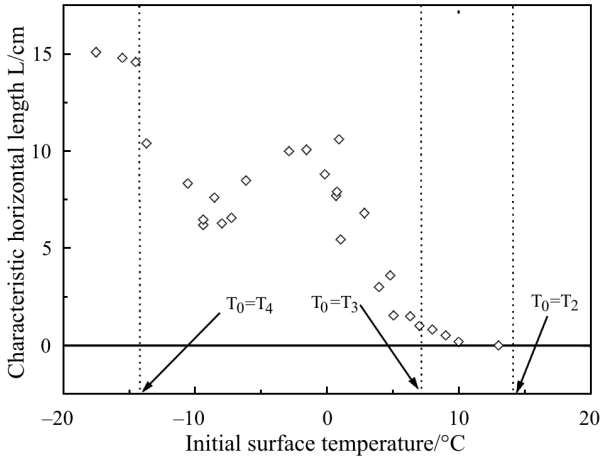

Fig. 17 Approximated horizontal length L of the vortex *vs.* initial temperature

Critical transition temperatures

For values $T_0>T_1$ the fuel vapour pressure is so high that the flame spreading is controlled by the gas phase, and the presence of the liquid fuel is ignored by the flame. For values $T_2<T_0<T_1$, a new uniform regime, controlled by heat diffusion in the liquid phase, appears. Therefore, T_1 should be considered as a steady state bifurcation. The slope of the T_0–v_f diagram in this region is of order 10 cm s^{-1} ºC^{-1}, while, for $T_3<T_0<T_2$, it is of order 1 cm s^{-1} ºC^{-1} as Fig. 11 shows. More detail can be found in Fig. 18, corresponding to ethanol in a 40 cm long channel, with lateral walls of Pyrex. Therefore, T_2 corresponds to a transcritical bifurcation. As the thermocouple records show, this transition temperature is the critical value flame propagation controlled (for $T_0>T_2$) by heat diffusion in the liquid turns (for $T_0<T_2$) to flame propagation assisted by heat convection (of characteristic size L) in the condensed phase.

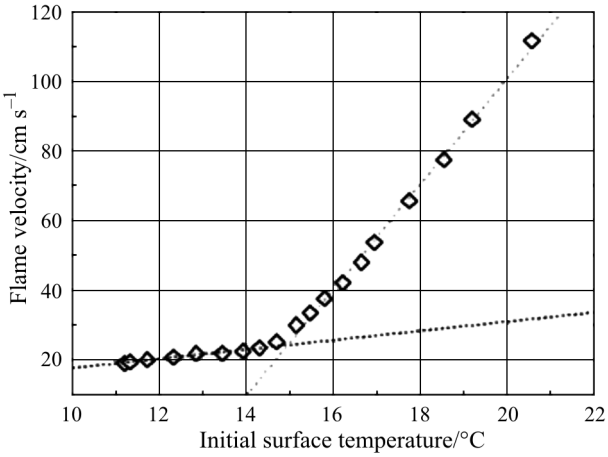

Fig. 18 Flame velocity *vs*. initial surface temperature (ethanol, 40 cm long channel, Pyrex)

The value T_3 is the threshold at which flame spreading proceeds with an oscillatory velocity. If we consider flame spreading as a dynamical system, by adopting $T=T_0$ as the external control parameter and the amplitude of the oscillatory part of the spreading velocity as an inner variable of the system, we can conclude that T_3 corresponds to a Hopf bifurcation. Theory predicts [12] that, for values slightly supercritical of the control parameter, the amplitude of the inner variable (the oscillation amplitude of the spreading velocity) and the oscillation frequency have to follow the dimensionless laws

$$\frac{v_f^{max} - v_f^{min}}{\bar{v}_f} = A\sqrt{\frac{T_3 - T_0}{T_3}}; \quad \frac{P - P_3}{P_3} = B\frac{T_3 - T_0}{T_3}$$

where the superscripts v_f^{max} and v_f^{min} refer to the maximum and the minimum values of the pulsation velocity, respectively, $\bar{v}_f$ is the average spreading velocity during the pulsation, P_3 is the oscillation period for the temperature T_3, and A, B are constants characterising the system. The predictions of these two relations have been compared with our experimental results: they are shown to be very well correlated by the precedent laws, as we can see in Fig. 19. In this figure, we combine two graphics. Lines represent the statistical linear fit between these variables, with T_3=5.8ºC, P_3=0.5 s, A=2.55, B=1.75.

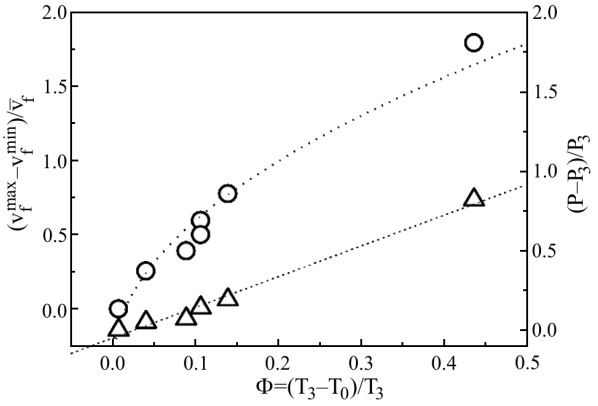

Fig. 19 ○ – Amplitude of the pulsation velocity and △ – the period around the critical point T_3

Finally we observe that, for $T_0=T_4$, the oscillation period diverges; this critical temperature is the transition value from the oscillation regime to a new low velocity steady state. Therefore, T_4 resembles a homoclinic point.

Table 1 shows the critical values obtained for ethanol in two different channels with lateral walls made of duralumin.

Comparing the experimental results for both channels we cannot conclude any dependence for T_1, T_2 and T_3; this is not the case of T_4, where a strong dependence on the channel length is found. The geometry of the channel may be at the origin of this critical temperature.

Table 1 Critical temperatures for ethanol in two different channels

Channel/cm	Temperature/°C			
	T_1	T_2	T_3	T_4
40	22.5	9.5	3.5	–4.5
100	22.2	10.8	5.8	–14.6

Conclusions

The complete sequence of flame spreading regimes over liquid alcohols has been experimentally observed. The uniform region description has been completed. The pulsating period has been successfully evaluated, and a new slow motion regime (corresponding to very low temperatures) has been observed. Four transition points T_1, T_2, T_3 and T_4 have been characterized. A preheated region of warm liquid ahead of the flame appears, and its characteristic size has been experimentally registered. This assistance mechanism created by the thermocapillary vortex observed in our experiments seems to be the responsibility of the flame oscillation, although no theoretical background supports our statement; it can be the subject of future analysis. The study of flame behavior for different channel dimensions (especially for fuel containers, where all the dimensions are of the same order) and for different boundary conditions can be the subject of future work.

This work has been partially sponsored under projects number PB94-0385 (DGICYT, Spain) and A0303 (Universidad Politécnica de Madrid, Spain).

Abbreviation

v_f	flame spreading velocity
x_f	flame front position
T_0	initial fuel surface temperature
ϕ	thermocouples diameter
N	sampling rate
T	surface temperature
$T_{1,2,3,4,5}$	critical transition temperatures of flame spreading
P	period oscillation
P_3	oscillation period corresponding to $T_0=T_3$
T_{flash}	flash point temperature of the liquid fuel
q_g	heat flux in the gas phase
λ_g	gas thermal conductivity
λ_l	liquid thermal conductivity
q_l	heat flux in the liquid phase
ΔT_l	temperature difference in the liquid phase

ΔT_g	temperature difference in the gas phase
T_b	fuel boiling temperature
T_f	flame temperature
δ_{nsg}	characteristic size of the Navier–Stokes region
δ_T	characteristic thermal size of the Navier–Stokes region
u_{nsg}	local velocity of the Navier–Stokes region
ρ_l, ρ	liquid density
μ_l	liquid viscosity
ρ_g	gas density
μ_g	gas viscosity
c_{pg}	gas heat capacity
c_{pl}	liquid capacity
Pr	Prandtl number
Re	characteristic channel flow Reynolds number
h	liquid fuel depth
σ	surface tension
χ_g	thermal gas diffusivity
u_s	characteristic velocity of the liquid under the flame position
L	characteristic horizontal length of the convection zone
S	dimensionless parameter u_s/v_f

References

1 K. Akita, Fourteenth Symposium (International) on Combustion, The Combustion Institute, Pittsburgh 1973, pp. 1075–1083.
2 W. A. Sirignano and I. Glassman, Combust. Sci. Tech., 1 (1970) 307.
3 I. Glassman and F. L. Dryer, Fire Safety J., 3 (1980) 123.
4 C. Di Blasi, S. Crescitelli and G. Russo, XXIII. Symposium (International) on Combustion, The Combustion Institute, Pittsburgh 1990, pp. 1669–1675.
5 A. Ito, D. Masuda and K. Saito, Combust. Flame, 83 (1991) 375.
6 F. J. Miller and H. D. Ross, 'Liquid-phase velocity and temperature fields during uniform flame spread over 1-propanol', 8th International Symposium on Transport Processes, San Francisco, CA 1995.
7 M. Furuta, J. Humphrey and A. C. Fernández-Pello, Phys. Chem. Hydrodynamics, 6 (1985) 347.
8 R. Mackinven, J. Hansel and I. Glassman, Comb. Sci. Technol., 1 (1970) 293.
9 R. Schiller, H. D. Ross and W. A. Sirignano, Combust. Sci. Technol., 118 (1996) 203.
10 H. D. Ross and R. G. Sotos, XXIII. Symposium (International) on Combustion, The Combustion Institute, Pittsburgh 1990, pp. 1649–1655.
11 J. M. Miller and H. D. Ross, XXIV. Symposium (International) on Combustion, The Combustion Institute, Pittsburgh 1992, pp. 1703–1711.
12 G. Nicolis, Introduction to Nonlinear Science (Cambridge University Press, Cambridge, MA 1995).